Silikáty 29, s. 21—30 (1985)

SINTERING MECHANISMS OF MgO

MIROSLAV HAVIAR, VILIAM FIGUSCH, ZDENĚK PÁNEK

Received 12. 9. 1983

The higher purity and higher calcining temperatures of the MgO *powder tend to retard the particle rearrangement process during the early stages of the sintering of* MgO *powder compacts. The neck growth between* MgO *particles is controlled by surface diffusion at the beginning of the sintering. With increasing temperature the transport mechanisms causing densification predominate over surface diffusion.*

INTRODUCTION

The sintering mechanisms of MgO were a frequent subject of the materials science research during past years. The aim of this effort was to understand the sintering process in ceramics and to prepare the materials of behaviour desired. Clark and White [1] comparing densification data with their equations for sintering model found viscous or plastic flow to be the active mechanisms. Brown [2] reported that bulk densities of very pure magnesia sintered at 1 300 to 1 500 °C were linearly proportional to ln t with the activation energy 113 kJ/mol. Reeve and Clare [3] reanalyzed these data and concluded that the true activation energy for diffusion should be $\approx$ 330 kJ/mol. This value is in good agreement with the activation energy for bulk diffusion of Mg in MgO [4]. Hashimoto et al. [5] reported consider-ably faster diffusion of oxygen along grain-boundaries in polycrystalline MgO than through the bulk. Wermuth and Knapp [6] found that during isothermal sintering experiments on MgO in dry N_2 the shrinkage was proportional to time to the 0.34 power, indicating agreement with the grain-boundary diffusion model. Wong and Pask [7] divided the sintering process into two steps. First one is the transport of mass from grain-boundary to the neck region and second one is further transport to the adjoining free surface regions. They found that during sintering of MgO in static air the second step was rate-controlling. Varela et al. [8] in recent study found that structural rearrangement of grains is present at the beginning of the sintering process of the MgO powder calcined at 900 °C.

From this brief review it can be seen that there is no agreement between authors dealing with sintering process of MgO. It is evident that there is often a large gap between real geometry of experimental powder compacts and model geometry used for the interpretation of sintering experiments. Further experiments by methods which provide parameters correlating with microstructural development of sintering compacts could contribute to better understanding of the phenomena occuring during sintering process.

In the present study the method of simultaneous measurement of shrinkage and electrical conductivity during the sintering process was used. With the help of suggested method the instant neck size can be calculated from the conductivity data. From the neck size the apparent shrinkage caused by the mechanisms contributing to shrinkage only (volume and grain-boundary diffusion) can be calculated.

Comparison of thus obtained shrinkage and the shrinkage experimentally measured allows us to determine the contribution of surface diffusion and evaporation — condensation to the total material transport to the neck region. For details of the method see [9].

EXPERIMENTAL

Commercial magnesia powders usually consist of aggregated particles and are not suitable for investigation designed. Therefore, procedure able to produce magnesia powder with uniform, individual grains of submicron dimensions was sought. The method of selective dissolution of CaO from calcined dolomite (dolomia) was selected. Magnesia occurs in dolomia grains (porosity $\approx$ 50 vol. %) in the form of mostly individual, equiaxed particles embedded in porous CaO matrix. Latter can be leached by reaction with suitable reagent in non-aqueous medium and magnesia particles, not participating in reaction are released. Two different MgO powders, labeled A and C, were prepared by method mentioned above from pure dolomia and dolomia recrystallized in the presence of LiCl flux, respectively. The calcination of dolomite was carried out at the temperature 1 300 °C for 2 hours.

Powder A

Calcium oxide was leached from dolomia by reaction with equivalent amount fo NH_4NO_3 in boiling *n*-buthanol (500 ml) according to scheme:

$$(CaO + MgO) + 2\,NH_4NO_3 \rightarrow Ca(NO_3)_2 + 2\,NH_3 + H_2O + MgO$$

The reaction was carried out in 1 liter 3-throat flask with mechanical stirrer and Soxhlet extraction apparatus filled with granular dolomia. Latter served as dessicator for water released during reaction. Ammonia was pumped from the top of the reflux cooler by water pump. The pressure in apparatus was held at appr. 30 kPa by admitting dry, CO_2 free air through a capillary into reaction mixture. After 5 hours refluxing the reaction mixture was hot-filtered. The filtration cake was thoroughly washed with methylalcohol, dried and calcined at 900 °C for 1 hour.

The composition of the powder labeled as A is given in the Tab. I.

Table I

Composition of the powder MgO—A by chemical analysis

Component	MgO	CaO	SiO_2	Al_2O_3	Fe_2O_3
wt. %	98,10	1,41	0,22	0,15	0,12

The powder consisted of individual grains with the narrow size distribution, 65 % of them being from the interval (100, 200) nm.

Powder C

In the case of powder C dolomia was recrystallized in the presence of LiCl flux. The calcinate was mixed with the solution of LiCl in methanol and dried to obtain a mixture containing 5 wt. % LiCl, pressed to tablets, heated up to 850 °C with 5 hours dwell at this temperature. The presence of LiCl flux causes grain growth in the powder. Calcium oxide was selectively leached from powdered calcinate

(30 g) by treating in ethyleneglycol (500 ml) at 70 °C in a closed flask. After 3 hours the reaction mixture was filtered, the cake washed with absolute ethanol, dried and finally calcined at 1 220 °C for 1 hour. The composition of the powder obtained is given in the Tab. II.

Table II

Composition of the powder MgO—C by spectral analysis

Mg	main component
Ca	0,05—0,1 %
Fe	0,01—0,05 %
B	0,01—0,05 %
Si	0,005—0,01 %
Cu	0,005—0,01 %
Mn	0,001—0.005 %

The powder also consisted of individual grains with the mean diameter of 250 nm. The SEM micrographs of the powders A and C are shown in Figs. 9, 10.

To improve an electrical contact thin layers of CeO_2 + 10 % MgO powder (0.02 mm) were applied to the flat surfaces of the pellets.

The experiments were carried out in high temperature dilatometer Netzsch, type 402 E which was provided for conductivity measurements with Pt — 30 % Rh disc electrodes. The conductance was measured in the range 10^{-2}—10^{-8} S using Semi-automatic bridge Tesla BM 484.

The experiments were carried out in constant heating rate regime with the subsequent temperature dwell, the rate of temperature rise being 10 K/min. The data of shrinkage, conductance and temperature were continually recorded. From the values of shrinkage and conductance the instant value of conductivity was calculated. From the conductivity data the instant neck size was calculated according to

$$\frac{x}{a} = \exp \frac{\frac{\sigma_0}{\sigma_m} - U}{V}, \tag{1}$$

where x is the neck radius, a the radius of the grains, σ_0 the conductivity of the dense sample, σ_m the conductivity of the sintering sample and U, V are constants equal to 0.7647 and —1.155, respectively. To obtain σ_0 the conductance of the sintered sample must be measured once more by use of identical temperature treatment. If the sample is not sintered to the theoretical density the conductivity must be corrected to zero porosity value

$$\sigma_0 = \sigma_0'(1 - p)^{-1}, \tag{2}$$

where σ_0' is the conductivity of the sintered sample and p is its porosity. From the neck size the apparent shrinkage (when the mechanisms contributing to shrinkage only are operative) can be calculated with use of fourth degree polynomial

$$\frac{\Delta l}{l_0} = A_0 + A_1 \frac{x}{a} + A_2 \left(\frac{x}{a}\right)^2 + A_3 \left(\frac{x}{a}\right)^3 + A_4 \left(\frac{x}{a}\right)^4, \tag{3}$$

where $A_0 = 0.00$; $A_1 = +0.0041$; $A_2 = +0.5082$; $A_3 = -0.1384$ and $A_4 = -0.0402$. For details of all these calculations see [9].

RESULTS AND DISCUSSION

The measured shrinkages and conductivity changes during the sintering of MgO — A are plotted in terms of $\Delta l/l_0$ and log $\frac{\sigma_m}{\sigma_0}$ vs. temperature resp. dwell time in Figs. 1—3. The microstructure of the sample sintered at 1 250 °C for 230 min. is shown in Fig. 11. On all curves of the conductivity changes the typical effects are present. These are marked on Fig. 2. From 600 to 800 °C there is a conductivity decrease (effect *I*), between 800 and 1 000 °C conductivity rises (effect *II*).

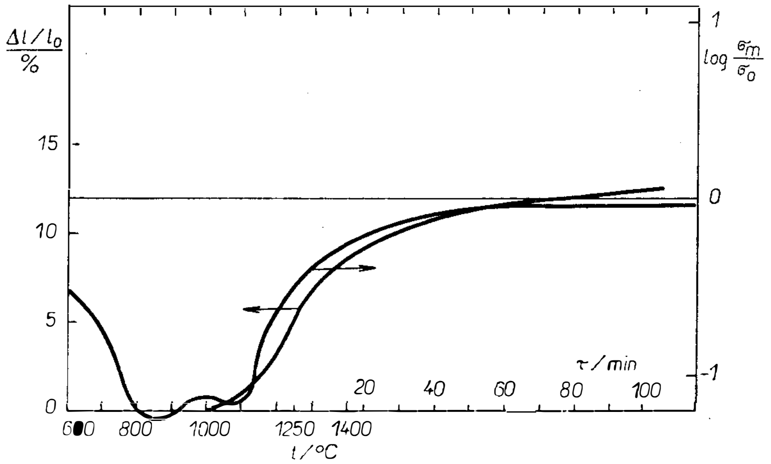

Fig. 1. Relative shrinkage $(\Delta l/l_0)_m$ *. 100 and conductivity change log* σ_m/σ_0 *of the sintered* MgO—A *powder. Sintering temperature 1 250 °C.*

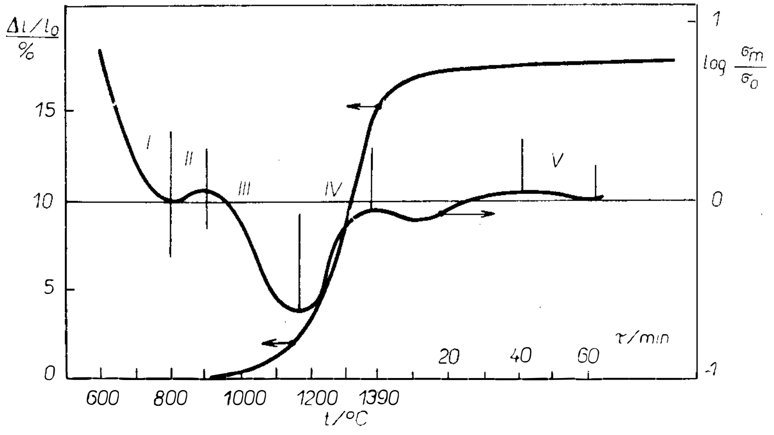

Fig. 2. Relative shrinkage $(\Delta l/l_0)_m$ *. 100 and conductivity change log* σ_m/σ_0 *of the sintered* MgO—A *powder. Sintering temperature 1 390 °C.*

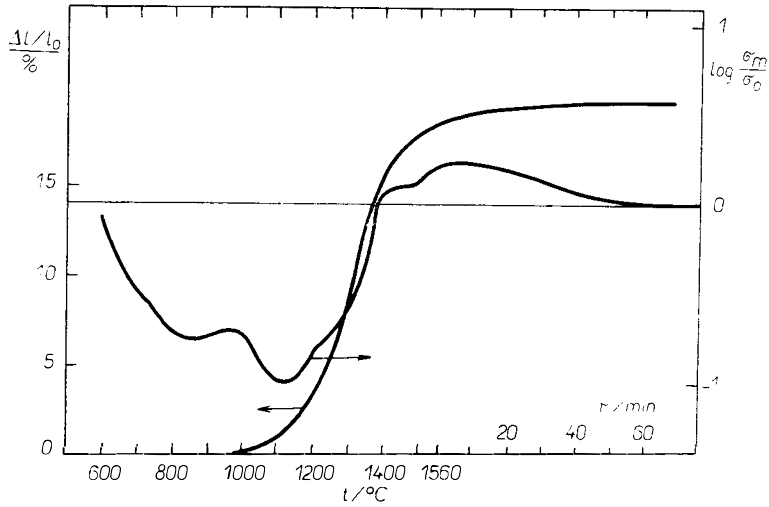

Fig. 3. Relative shrinkage $(\Delta l/l_0)_m$ *. 100 and conductivity change log* σ_m/σ_0 *of the sintered* MgO—A *powder. Sintering temperature 1 560 °C.*

Over 1 000 °C there is again a decrease (effect *III*), over 1 100 °C there is a rise (effect *IV*) interrupted at 1 350 °C by a slight decrease. During the sintering at higher temperatures there is a conductivity decrease at the end of the sintering process.

The preliminary decrease (effect *I*) was reported also by Vorobyov et al. [10]. The decrease is caused by gas desorption from free surfaces. The desorption of gases trapped at the surfaces causes decreasing of the surface conductivity. The effects *II* and *IV* (conductivity increase) are due to the neck growth between the sintering grains. This process changes the effective cross section area of the sample which results in incresing conductivity. The conductivity drop at cca 1 000 °C is caused by surface hydroxide layer decomposition. This observation is in good agreement with study of Anderson at al. [11]. The hydroxide has higher conductivity and interruption of such a layers results in conductivity decrease. As is clearly seen from Figs. 1—3, this effect has various intensity. This is due to the various stage of the hydratation of the powder. All powders were held in dessicator. During the preparation of the sample it was practically impossible to keep reproducible conditions (various duration of the preparation and various humidity). This could influence various stage of hydratation of the powder.

From the conductivity increase (effects *II* and *IV*) of the sample sintered at 1 250 °C apparent shrinkage was calculated. Latter values and the measured shrinkages are shown in Fig. 4. The measured shrinkages are at the beginning of the process greater than apparent ones indicating that there was no neck growth between the sintering grains. Thus, the densification was caused by structural rearrangement of the grains. This process is dependent upon quality of the grain's surfaces and was not present in the sintering process of the powder C. This was calcined at higher temperature (1 220 °C) than powder A (900 °C) and its purity was also significantly higher (compare Tabs. I and II). It is difficult to judge whether the presence of impurities or the lower calcination temperature (or both) are responsible for the rearrangement process.

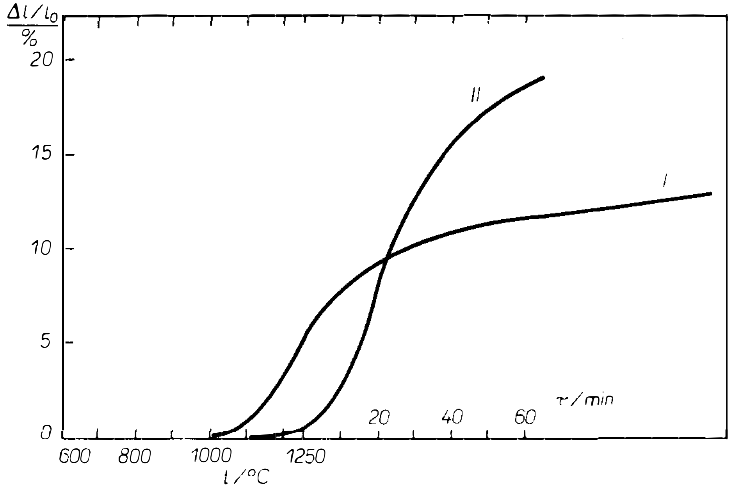

Fig. 4. Relative shrinkage of the powder MgO—A *sintered at 1 250 °C. I — measured shrinkage, II — apparent shrinkage determined from the conductivity data.*

In further course of the sintering process the apparent shrinkage is greater than the shrinkage experimentally measured indicating the activity of nondensifying mechanisms.

The slight decrease of the conductivity at the end of the sintering process is due to the grain growth and subsequent decrease of the free surfaces and grain-boundaries area.

Powder C showed lower sintering rates and another conductivity changes than powder A. These are due to the higher purity of the powder C. The course of the hrinkage and conductivity changes are shown in Figs. 5—6, the microstructure

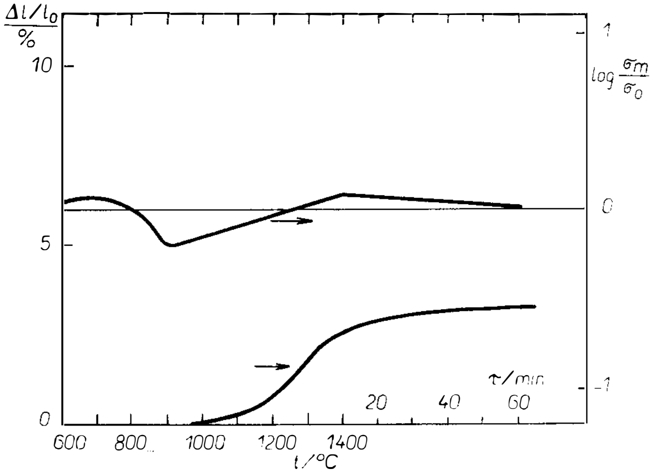

Fig. 5. Relative shrinkage $(\Delta l/l_0)_m$ *. 100 and conductivity change log* σ_m/σ_0 *of the sintered* MgO—C *powder. Sintering temperature 1 300 °C.*

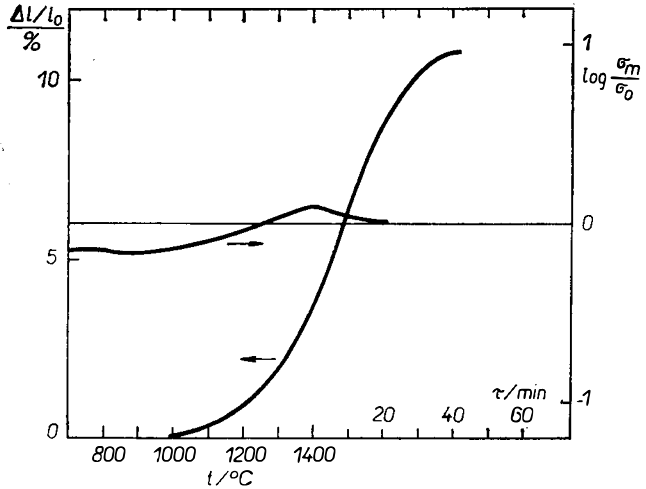

Fig.6. Relative shrinkage $(\Delta l/l_0)_m$ *. 100 and conductivity change log* σ_m/σ_0 *of the sintered* MgO—C *powder. Sintering temperature 1 400 °C.*

of the sample sintered at 1 300 °C for 60 min in Fig. 12. The powder was calcined at higher temperature —1 220 °C, so one can suppose that to the gas desorption and release of the surface hydroxide layer came during the calcination process. The conductivity decrease up to 900 °C of the sample sintered at 1 300 °C (Fig. 5 can be explained by partial hydratation of the powder. The pellet for the experiment at 1 300 °C was prepared after that sintered at 1 400 °C so the powder was longer in contact with air humidity.

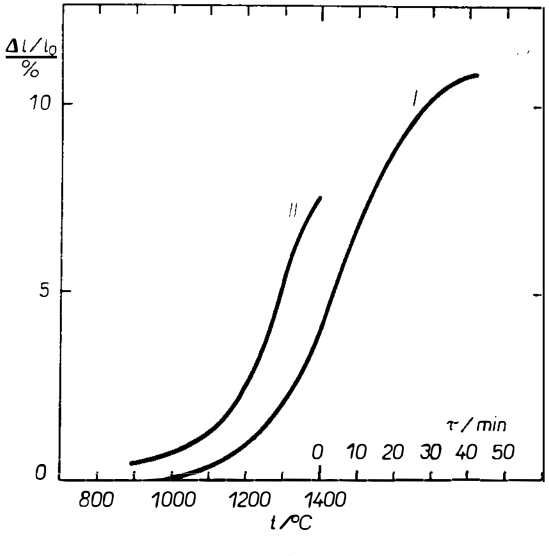

Fig. 7. Relative shrinkage of the powder MgO—C *sintered at 1 400 °C. I — measured shrinkage, II — apparent shrinkage determined from the conductivity data.*

As is clearly seen in Figs. 10 and 12, in the powder C no grain growth is present during the sintering at 1 300 °C, in contrary to the powder A. From the conductivity increase of the sample sintered at 1 400 °C the instant neck size and apparent shrinkage were calculated. This and the measured shrinkages are shown in Fig. 7. The contribution of nondensifying mechanisms (CNM) can be than calculated as

$$CNM = \frac{\left(\frac{\Delta l}{l_0}\right)_a - \left(\frac{\Delta l}{l_0}\right)_m}{\left(\frac{\Delta l}{l_0}\right)_a}. \qquad (4)$$

Thus obtained CNM values are plotted in Fig. 8. The contribution of nondensifying mechanisms (in the studied temperature range it is mainly surface diffusion) is at the beginning of the process (900 °C) close to 100 %, with increasing temperature and continuing shrinkage the percentage of CNM decreases. The surface diffusion ceases to be a dominant process at 1 300 °C. This suggests the lower activation energy of surface diffusion compared to the volume and grain-boundary diffusion [12].

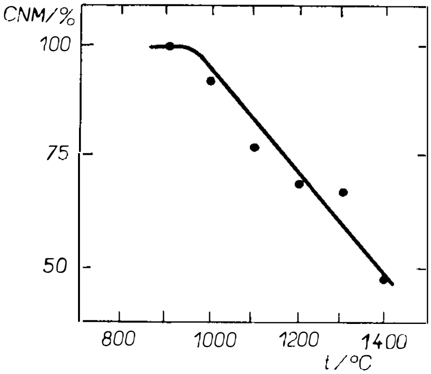

Fig. 8. Contribution of surface diffusion to mass transport to the neck regions during sintering of the powder MgO—C.

The reasons for the conductivity decrease at the end of experiment are probably the same as in the powder A, i.e. decrease of the free surface and grain-boundary area.

CONCLUSIONS

The desired aim in the preparation of sintered magnesia is to prepare the MgO as dense as possible. The knowledge of the contribution of nondensifying mechanisms (surface diffusion) to the sintering process can provide the effective method to reach this goal. This means to designe the heating curve with the maximal rate in the temperature region where surface diffusion is operative. The suggested method let us to determine this parameter of the sintering process.

By the method of simultaneous measurement of shrinkage and conductivity of the sintering sample the processes accompanying sintering were analyzed. It was found that during the heating of the powder A (purity 98.11 %, calcination temperature 900 °C) the surface layer of hydroxide is decomposed at cca 1 000 °C. At the beginning of the sintering process there is a significant particle rearrangement caused probably by the presence of the liquid phase. The powder C (purity 99.7 %, calcined at 1 220 °C) showed no particle rearrangement. The mechanism of the neck growth is surface diffusion at the beginning, its percentage deceases with increasing temperature and continuing shrinkage. This shows the lower value of activation energy of surface diffusion compared with that of volume and grain-boundary diffusion.

References

[1] Clark P. W., White J.: Trans. Br. Ceram. Soc., *49*, 305 (1950).
[2] Brown R. A.: Am. Ceram. Soc. Bull., *44*, *483* (1965).
[3] Reeve K. D., Clare T. E.: J. Am. Ceram. Soc., *49*, 400 (1966).
[4] Harding B. C., Price D. M., Phil. Mag., *26*, 253 (1972).
[5] Hashimoto H., Hama M., Shirasaki S.: J. Appl. Phys., *43*, 4828 (1972).
[6] Wermuth F. R., Knapp W. J.: J. Am. Ceram. Soc., *57*, 401 (1973).
[7] Wong. B., Pask J. A.: J. Am. Ceram. Soc., *62*, 141 (1979).
[8] Varela J. A., Whittemore O. J.: ibid., *66*, 77 (1983).
[9] Haviar M.: Ph. D. Thesis, Institute of Inorganic Chemistry, Chemical Research Centre, Slovak Academy of Sciences, Bratislava (1983).
[10] Vorobyov V. K., Poluboyarinov D. N., Bakunov V. S.: Ogneupory, No. 9, 40 (1971).
[11] Anderson P. J., Horlock R. F., Oliver J. F.: Trans. Faraday Soc., *61*, 2754 (1965).
[12] Johnson D. L.: *Sintering and Related Phenomena*, ed. Kuczynski G. C. Plenum Press, New York 1973, p. 363.

MECHANIZMY SPEKANIA MgO

Miroslav Haviar, Viliam Figusch, Zdeněk Pánek

Ústav anorganickej chémie CCHV SAV, 842 36 Bratislava

V práci sa vyšetrovali mechanizmy spekania MgO pomocou simultánneho merania zmraštenia a elektrickej vodivosti spekajúcej vzorky. Z nameranej vodivosti sa vypočítala veľkosť krčkov, veľkosti krčkov bolo priradené zmraštenie, ku ktorému by došlo, keby boli účinné len mechanizmy prispievajúce k zmrašteniu (objemová difúzia a difúzia po hraniciach zŕn). Porovnaním takto určeného zmraštenia a zmraštenia skutočne pozorovaného je možné určiť podiel mechanizmov neprispievajúcich k zmrašteniu na procese spekania.

Prášky MgO (označené A a C) sa pripravili selektívnym lúžením CaO z kalcinovaného dolomitu. Prášok A (obr. 9) bol čistoty 98.1 %, kalcinovaný bol pri teplote 900 °C, prášok C (obr. 10) mal čistotu 99.7 % a kalcinovaný bol pri teplote 1 220 °C.

Zistilo sa, že na počiatku procesu spekania prášku A dochádza k reorganizácii častíc. Intenzita tohto procesu je závislá na kvalite povrchov zrn prášku. V prípade prášku A je reorganizácia spôsobená buď prítomnosťou nečistôt alebo horšou kvalitou povrchov. Reorganizácia častíc sa počas spekania prášku C nevyskytuje. Na počiatku procesu spekania prášku C (pri teplote 900 °C) predstavuje povrchová difúzia takmer 100 % z celkového transportu látky do oblasti krčkov, s rastom teploty a pokračujúcim zmraštením jej podiel klesá. Povrchová difúzia prestáva byť dominantnou pri cca 1 300 °C. Svedčí to o nižšej aktivačnej energii povrchovej difúzie v porovnaní s objemovou difúziou a difúziou po hraniciach zŕn.

Obr. 1. Relatívne zmraštenie $(\Delta l/l_0)_m$ *. 100 a zmena konduktivity log* σ_m/σ_0 *spekajúceho prášku* MgO—A. *Teplota spekania 1 250 °C.*

Obr. 2. Relatívne zmraštenie $(\Delta l/l_0)_m$ *. 100 a zmena konduktivity log* σ_m/σ_0 *spekajúceho prášku* MgO—A. *Teplota spekania 1 390 °C.*

Obr. 3. Relatívne zmraštenie $(\Delta l/l_0)_m$ *. 100 a zmena konduktivity log* σ_m/σ_0 *spekajúceho prášku* MgO—A. *Teplota spekania 1 560 °C.*

Obr. 4. Relatívne zmraštenie prášku MgO—A *spekaného pri 1 250 °C. I — namerané zmraštenie, II — zdanlivé zmraštenie určené zo zmeny konduktivity.*

Obr. 5. Relatívne zmraštenie $(\Delta l/l_0)_m$ *. 100 a zmena konduktivity log* σ_m/σ_0 *spekajúceho prášku* MgO—C. *Teplota spekania 1 300 °C.*

Obr. 6. *Relatívne zmraštenie* $(\Delta l/l_0)_m$. *100 a zmena kondųktivity log* σ_m/σ_0 *spekajúceho prášku* MgO—C. *Teplota spekania 1 400 °C.*

Obr. 7. *Relatívne zmraštenie prášku* MgO—C *spekaného pri 1 400 °C. I — namerané zmraštenie, II — zdanlivé zmraštenie určené zo zmeny konduktivity.*

Obr. 8. *Príspevok povrchovej difúzie k transportu hmoty do oblasti krčkov počas spekania prášku* MgO—C.

Obr. 9. *Prášok* MgO—A.

Obr. 10. *Prášok* MgO—C.

Obr. 11. MgO—A *spekané pri 1 250 °C, 230 min.*

Obr. 12. MgO—C *pri teplote 1 300 °C, 60 min.*

МЕХАНИЗМЫ СПЕКАНИЯ MgO

Мирослав Гавиар, Вилиам Фигуш, Зденек Панек

Институт неорганической химии ЦХИ САН, 842 36 Братислава

В работе рассматриваются результаты исследования механизмов спекания MgO с помощью одновременных измерений усадки и электропроводности скекающегося образца. Из измеренной проводимости расчитали величину шеек, величину шеек соотносили к усадке ,которая наступила бы в случае действия только механизмов, которые помогают усадке (диффузия в объеме и диффузия по границам зерен). Сопоставляя таким образом установленную усадку с действительно наблюдаемой усадкой, можно выделить долю механизмов, не помогающих усадке, в процессе спекания.

Порошки MgO (обозначенные через A и C) приготовили селективным выщелачиванием CaO из кальцинированного доломита. Порошок A (рис. 9) чистотой 98,1 % кальцинировали при температуре 900 °C, порошок C (рис. 10) чистотой 99,7 % кальцинировали при температуре 1 220 °C.

Установили, что в начале процесса спекания порошка A происходит перераспределение частиц. Интенсивность данного процесса зависит от качества поверхностей зерен порошка. В случае порошка A перераспределение вызывается или присутствием загрязнений или низшим качеством поверхностей. Перераспределение частиц в течение спекания порошка C не встречается. В начале процесса спекания порошка C (при температуре 900 °C) представляет собой поверхностная диффузия почти 100 % общего транспорта вещества в область шеек, с ростом температуры и продолжающейся усадкой ее доля понижается. Поверхностная диффузия теряет доминирующее положение приблизительно при 1300 °C. Это является свидетельством более низкой энергии активации поверхностной диффузии в сопоставлении с диффузией в объеме и диффузией по границам зерен.

Рис. 1. *Относительная усадка* $(\Delta l/l_0)m$. *100 и изменение удельной проводимости* log σ_m/σ_0 *спекающегося порошка* MgO—A. *Температура спекания 1250 °C.*

Рис. 2. *Относительная усадка* $(\Delta l/l_0)m$. *100 и изменение удельной проводимости* log σ_m/σ_0 *спекающегося порошка* MgO—A. *Температура спекания 1390 °C.*

Рис. 3. *Относительная усадка* $(\Delta l/l_0)m$. *100 и изменение удельной проводимости* log σ_m/σ_0 *спекающегося порошка* MgO—A. *Температура спекания 1560 °C.*

Рис. 4. *Относительная усадка порошка* MgO—A, *спекающегося при температуре 1250 °C:* I — *измеренная усадка,* II — *кажущаяся усадка, установленная на основании изменения удельной проводимости.*

Рис. 5. *Относительная усадка* $(\Delta l/l_0)m$. *100 и изменение удельной проводимости* log σ_m/σ_0 *спекающегося порошка* MgO—C. *Температура спекания 1300 °C.*

Рис. 6. *Относительная усадка* $(\Delta l/l_0)m$. *100 и изменение удельной проводимости* log σ_m/σ_0 *спекающегося порошка* MgO—C. *Температура спекания 1400 °C.*

Рис. 7. *Относительная усадка порошка* MgO—C, *спекающегося при температуре 1400 °C:* I — *измеренная усадка,* II — *кажущаяся усадка, установленная на основании изменения удельной проводимости.*

Рис. 8. *Доля поверхностной диффузии к транспорту массы в область шеек во время спекания порошка* MgO—C.

Рис. 9. *Порошок* MgO—C.

Рис. 10. *Порошок* MgO—C.

Рис. 11. MgO—A, *спекающийся при температуре 1250 ° C, время 230 мин.*

Рис. 12. MgO—C, *спекающийся при температуре 1300 °C, время 60 мин.*

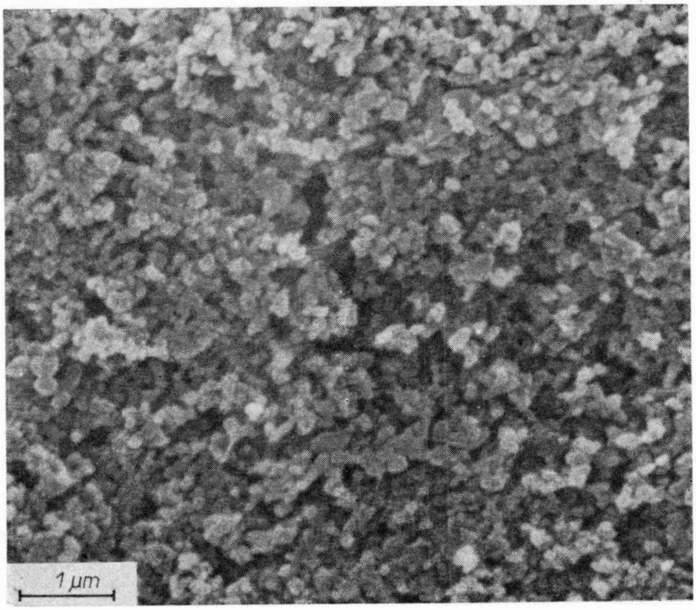

Fig. 9. Powder MgO—A.

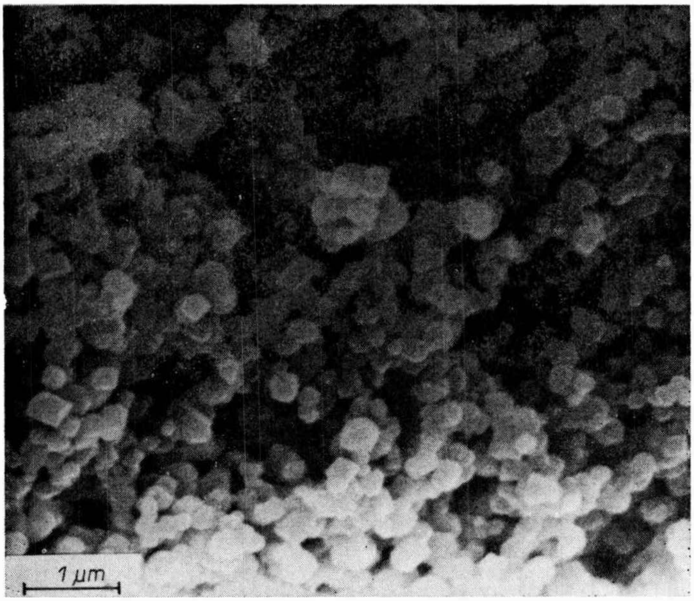

Fig. 10. Powder MgO—C.

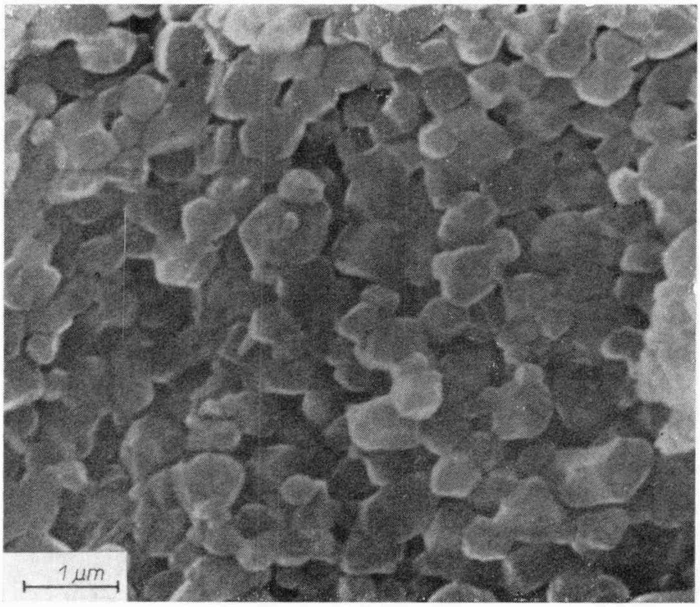

Fig. 11. MgO— A *sintered at 1 250 °C, 230 min.*

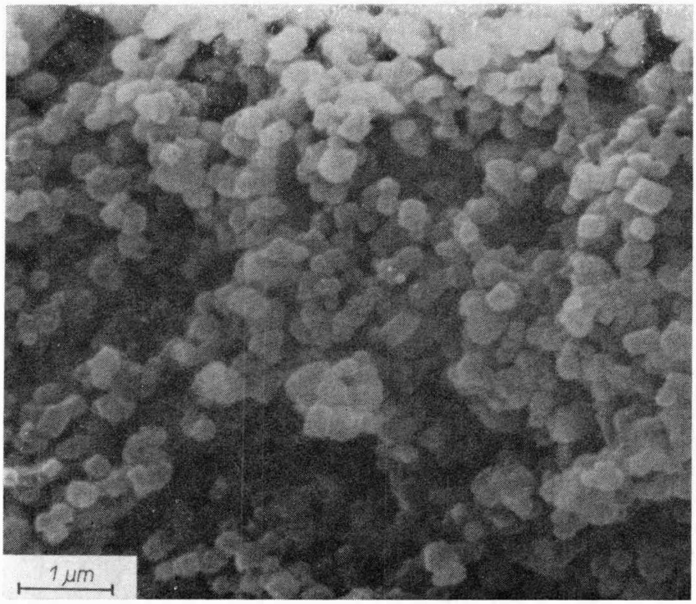

Fig. 12. MgO—C *at temperature 1 300 °C, 60 min.*